Proceedings of the 28th IEEE
EMBS Annual International Conference
New York City, USA, Aug 30-Sept 3, 2006

A Detection Scheme for Frontalis and Temporalis Muscle EMG Contamination of EEG Data

Michael J. Fu*, Janis J. Daly†, M. Cenk Çavuşoğlu‡

*Department of Electrical Engineering and Computer Science, Case Western Reserve University, Cleveland, Ohio 44106
Email: mjfu@case.edu
†Department of Neurology, Case Western Reserve University School of Medicine, Cleveland, Ohio 44106
Stroke Motor Control, Motor Laboratory, and FES Center of Excellence, LSCDVA Medical Center, Cleveland Ohio 44106
Email: jjd17@case.edu
‡Department of Electrical Engineering and Computer Science, Case Western Reserve University, Cleveland, Ohio 44106
Email: cavusoglu@case.edu

Abstract— **Electroencephalogram (EEG) recordings are highly susceptible to noise from electromyogram (EMG) signals of the frontalis and temporalis muscles. In this paper, we propose and evaluate a new method for detecting frontalis and temporalis muscle EMG contamination in EEG signals based on recent findings on topographic and spectral characteristics of cranial EMG.**

I. Introduction

Electroencephalogram (EEG) recording devices are designed to greatly amplify minuscule perturbations of electric potential, and as such, are extremely susceptible to noise. These artifacts can be caused by events such as inconsistencies in the power supply, the shifting of electrodes, and electromagnetic fields generated by nearby electronics. While there exist tools and methods to prevent many equipment-related noise sources from maligning data, artifacts caused by the subject's own muscles, such as electro-oculargram (EOG) and electromyogram (EMG) signals, still pose a challenge to both detect and remove.

In the 1980s, efforts at detecting and removing EEG artifacts focused on EOG caused by eye twitching or blinking. EOG can be recorded from the ocular muscles and visually or automatically detected [1]–[3]. Once detected, trials containing EOG artifacts can either be rejected from analysis or removed by various techniques. Recent methods for removing the effects of EOG artifacts involve wavelet analysis [4] and blind source separation using principal and independent component analysis [5], [6].

Scalp muscle EMG signals are another source of unwanted EEG artifacts. However, unlike EOG artifacts, dedicated measurements are not available to detect scalp EMG activity because the muscles responsible for the noise are in the direct path between EEG electrodes and the brain. Techniques similar to those used to remove EOG artifacts have been applied to remove EMG artifacts, but those that filter or attempt to correct the EEG data will inevitably distort the original signals [7]. Also, artifact-correcting methods are effective in reducing the undesired effects of artifacts, but there are cases when it is more preferable to detect and reject contaminated data.

The motivation for the currently proposed detection scheme was the study of motor planning EEG from stroke survivors with arm-related motor deficits. The subjects (some of whom did not receive prior rehabilitation therapy) were studied while performing rehabilitative arm-reach movement. During data collections, the subjects who struggled to perform the motor task were observed to have exhibited strained facial expressions or teeth clenching. Previous methods for studying EEG in stroke survivors excluded subjects who could not successfully perform the studied motor tasks [8], [9]. However, when rehabilitative motor tasks are studied, subjects cannot be expected to be adept at the studied motor task. In such cases, it is not always possible for subjects to avoid unnecessary facial movements and trials containing EMG contamination are likely to exist.

Also, there is evidence that stroke infarcts change EEG characteristics during motor planning, but the extent of the changes is not yet well understood [10]. Therefore, to study the distortion of EEG data from stroke infarcts, it is important to minimize signal processing distortion during data analysis. For this reason, we decided against applying artifact removal or filtering schemes to our data. Ideally, we wanted to analyze only the artifact-free EEG data and ignore any contaminated data.

Classical methods of artifact detection involve visual or automated inspection for data that exceeds a pre-defined amplitude threshold [11]. This approach works well for EOG artifacts, which can be measured by electrodes placed around the ocular muscles. EMG activity, on the other hand, exists between 0–200 Hz and is difficult and time-consuming to accurately identify by visual inspection. Computer-assisted artifact detection methods were proposed in the 1990s by Joutsiniemi *et al.* [12] and Brunner, *et al.* [13]. Joutsiniemi *et al.* proposed a neural network algorithm applied to 22-channel EEG recordings. Brunner, *et al.* used activity in the 26.25–32 Hz frequency band to reject artifacts for sleep EEG studies. In 2003, detailed information on cranial EMG, which

1-4244-0033-3/06/$20.00 ©2006 IEEE.

did not previously exist, was introduced by Goncharova, *et al.* [14]. Goncharova, *et al.* studied cranial EMG spectral and topographical characteristics in order to improve the understanding of this topic and aid in EMG artifact detection and removal. In 2005, Gasser *et al.* proposed a method to correct EEG data based on activity in the 51–69 Hz frequency "muscle-band" of EEG electrode F7. It is possible to use the muscle-band for EMG detection, but methods based on Goncharova *et al.*'s findings dedicated to EMG artifact detection still do not yet exist.

A. Study Objectives

We designed a scheme for detecting frontalis and temporalis muscle EMG activity based on the topographic and spectral data for these muscles that was reported by Goncharova *et al.* [14] and the subject's baseline, EMG-free data. We also characterized the robustness of our detection scheme when baseline data was not available and the detection thresholds were computed from EMG-contaminated data.

B. Paper Outline

First, we describe the data collection methods used to obtain muscle EMG activity in EEG data. Then we present the EMG-detection scheme and the selection of critical parameters based on a subject's baseline, EMG-free EEG data. Next, we characterized the robustness of our methods when the detection thresholds were computed using data with various levels of EMG contamination. Finally we cover applications for this detection scheme and future work.

II. Methods

A. Subject

One healthy adult male, age 24, gave consent to participate in this experiment. This study was conducted according to the Declaration of Helsinki and oversight was provided by the Internal Review Board of the Louis Stokes Cleveland Veterans Affairs Medical Center.

B. Experiment Paradigm

The subject was seated before a computer screen with his right (dominant) hand gripping the end-effector of an Interactive Motion Technologies Inc. (Cambridge, MA) Inmotion^2 Shoulder Elbow Robot. To standardize the movement, the subject was then presented with a motor targeting task that required an accurate 14 cm, linear movement in the horizontal plane beginning at the center of the workspace and reaching to a target in a direction directly in front of the subject. This motor task required shoulder flexion and elbow extension

Three types of EEG data were recorded from the subject. First, 40 trials of EMG-free data were recorded with the subject refraining from moving any facial muscles while performing the motor task. Then, 25 trials of frontalis muscle EMG-contaminated data were recorded by having the subject raise his eyebrows while performing the motor task. Finally, 20 trials of frontalis and temporalis muscle (fronto-tempo) EMG-contaminated data were recorded by having the subject both move his eyebrows and clench his teeth while performing the motor task.

C. Data Acquisition

EEG data was obtained using Compumedics NeuroScan Ltd. (El Paso, TX) devices and software. The data was recorded using Acquire 4.3.1 software, a 64-electrode QuickCap EEG cap, and a Synamps amplifier system (500 gain, sampling rate of 1000 Hz). All electrodes on the EEG cap were 8 mm in diameter with a 5 mm cavity depth and were arranged on the scalp in compliance with the International 10-20 standard [15]. Each recording was referenced to the common linked left and right mastoid surface electrodes. All electrode-to-scalp impedances were reduced to less than 10 kΩ using electrically conductive gel and real-time electrode impedance measurements provided by the Acquire software. Any eye-blink artifacts were removed by visual inspection. What remained was 31 EMG-free trials, 19 fronatlis-contaminated trials, and 12 fronto-tempo-contaminated trials (62 total trials). We also applied spatial filtering to EEG to improve the signal-to-noise ratio (SNR) as described in the next subsection.

D. Spatial Filtering

Using NeuroScan Edit 4.3.1, a common average reference (CAR) was performed on all 64 electrodes in order to produce a "reference-free" version of the EEG data. CAR was chosen base on its superior SNR characteristics as reported in a study performed by McFarland *et al.*, which compared several spatial filtering techniques for improving the SNR of EEG signals for BCI use and concluded that the CAR had the best SNR [16]. In the calculation of the CAR, the average value of all 64 electrodes is subtracted from the channel of interest for each sample of data. Specifically, the formula for CAR was:

$$V_i^{CAR} = V_i^{ER} - \frac{1}{64}\sum_{j=1}^{64} V_j^{ER} \quad (1)$$

where $V_i{}^{ER}$ is the potential between the *i*th electrode and the reference electrode. The effect of the CAR spatial filter was that any noise common to all the electrodes was removed from the EEG data.

III. EMG Artifact Detection

The following algorithm for EMG detection were largely based on the findings by Goncharova, *et al.* on the characteristics of frontalis and temporalis muscle EMG signals as measured through EEG recording equipment [14].

A. Frontalis and Temporalis EMG Characteristics

Spectrally, the frontalis muscle (which moves the eyebrows) exhibit maximum EMG activity from 16–38 Hz and the temporalis muscles (which are contracted when teeth are clenched) have maximum EMG activity from 13–34 Hz. However, both frontalis and temporalis muscles also have secondary peaks between 45–70 Hz. The 45–70 Hz frequency band is more suitable for EMG detection because

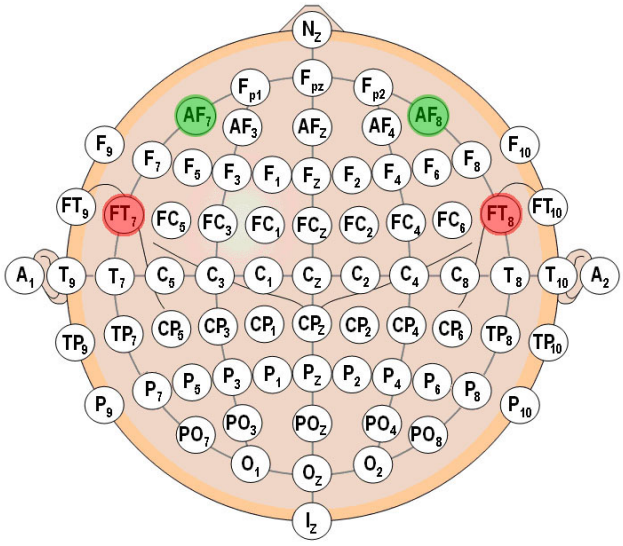

Fig. 1. The shaded circles are the locations of AF7 and AF8 (affected most by frontalis muscle activity) and FT7 and FT8 (affected most by temporalis muscle activity) on the 64-electrode International 10-20 EEG electrode placement standard used in this study [17].

in this range, EEG signal amplitudes are much smaller compared to the EEG signal amplitudes between 13–38 Hz. Therefore, peaks that occur between 45–70 Hz will most likely be from EMG activity.

Spatially, electrodes AF7 and AF8 are most affected by the frontalis muscle and electrodes FT7 and FT8 are most affected by the temporalis muscles (Fig.1). We will refer to AF7, AF8, FT7, and FT8 as the "primary" electrodes. Also, when the electrodes adjacent to the primary electrodes are affected by EMG, they reflect similar spectral characteristics with only slightly diminished amplitudes.

B. Detection Methods

At the primary electrodes, the 45–70 Hz frequency band power was computed in each trial and analyzed for abnormally high amplitudes. Scalp muscle EMG exhibits peaks in this frequency band, but EEG signals do not.

The power was calculated using the formula:

$$Power_{45-70Hz} = \frac{1}{N^2} \sum_{k=\frac{45N}{f_s}}^{\frac{70N}{f_s}} (|X(k)|^2 + |X(N-k)|^2) \quad (2)$$

where *N* is the total number of samples in the time interval of interest and *X(k)* is the *k*th Discrete Fourier Transform coefficient, and f_s is the sampling frequency.

Next, for each electrode, we calculated mean plus one standard deviation of the 45–70 Hz bandpower from EMG-free baseline trials and defined this as the "detection threshold" (The selection of this threshold will be explained in the following section). For each trial, if the 45–70 Hz band power for a primary electrode exceeded the detection threshold, then we examined five electrodes overlaying the muscles of interest and adjacent to that primary electrode. Goncharova, *et al.* reported that frontalis and temporalis EMG activity

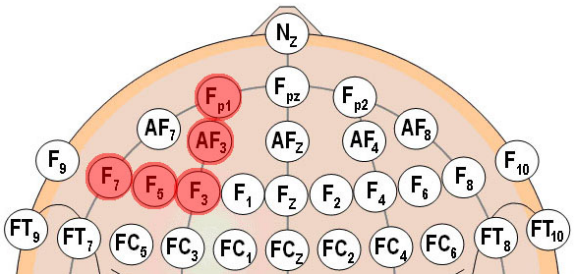

Fig. 2. If AF7 showed 45–70 Hz bandpower exceeding the detection threshold for a particular trial, then five adjacent electrodes (shaded circles) are further examined.

should affect the region around the primary electrodes, so the electrodes adjacent to the primary electrodes were analyzed to affirm the existence of EMG activity and prevent false detections. The adjacent electrodes for AF7 were FP1, AF3, F3, F5, and F7. The adjacent electrodes for FT7 were F7, F9, FT9, FC5, and T7. Similarly, the adjacent electrodes for AF8 were FP2, AF4, F4, F6, and F8. And the adjacent electrodes for FT8 were F8, F10, FT10, FC6, and T8. We examined the adjacent electrodes to see how many of them also had 45–70 Hz power values from the same trial that exceeded the detection threshold. Finally, if three of the five adjacent electrodes had power values that exceeded the detection threshold, then the trial was suspected of containing EMG artifacts. The reason for selecting three electrodes as the "decisive number" is explained in the following section.

For example, if during trial number 4, electrode AF7 had 45–70 Hz band power greater than the detection threshold, then data at electrodes FP1, AF3, F3, F5, and F7, (Fig. 2) from the same trial was also analyzed. If three of these five electrodes also exhibited power values for the suspected trial that exceeded the detection threshold for each respective electrode, then trial number 4 was identified to have had EMG contamination.

C. Parameter Selection

There are two variable parameters in our detection scheme: the decisive number and the detection threshold.

Mean plus one standard deviation was selected as the detection threshold as determined using the 31 EMG-free trials. Rejecting trials outside this threshold was expected to preserve approximately 80% of EMG-free data and rejected approximately 80% of frontalis contaminated data, and more than 90% of fronto-tempo-contaminated data. These observations were made from Fig. 3, which shows a histogram of 45–70 Hz bandpower during rest, frontalis activation, and frontalis and temporalis activation for the FZ electrode. The FZ electrode was analyzed for the threshold selection because of its central location between the primary electrodes that were analyzed for EMG activity.

To select the decisive number, the detection methods were applied to the 62 total trials (31 EMG-free, 19 frontalis-contaminated, and 12 fronto-tempo-contaminated) using 0–5 neighboring electrodes and detection thresholds computed

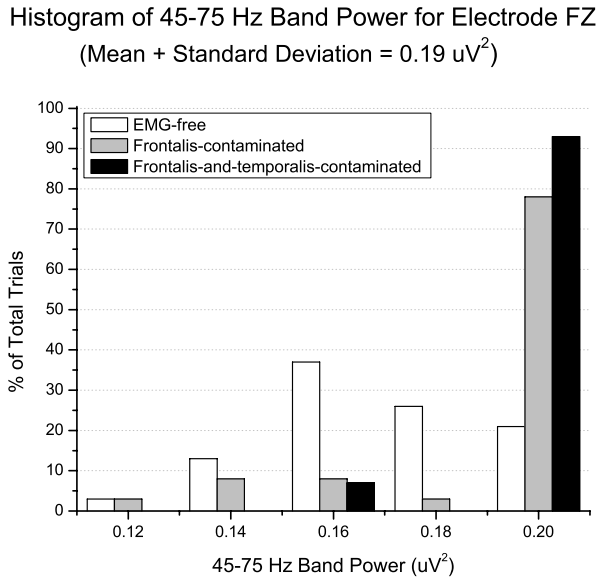

Fig. 3. This histogram shows the distributions of 45–70 Hz band power from all the trials of EMG-free EEG (white), frontalis-contaminated EEG (gray), and frontalis and temporalis-contaminated EEG (black). The mean and standard deviation were computed only from the EMG-free trials. We can see that only 20% of the EMG-free data lies beyond the mean plus one standard deviation, but 80% of frontalis-contaminated data and 90% of fronto-tempo-contaminated data lies beyond this threshold.

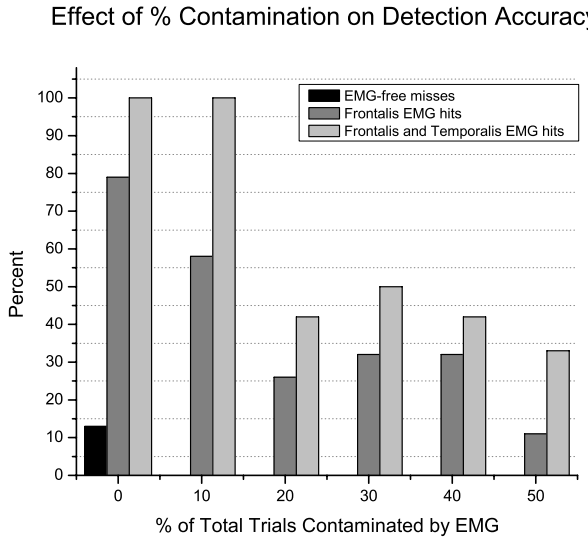

Fig. 4. To characterize the effect of contamination on the detection accuracy of our scheme when EMG-free baseline data was not available, we computed means and standard deviations assuming 10, 20, 30, 40, and 50% of the trials in a dataset were contaminated. The black bar shows the percent of EMG-free trials mistakenly identified to be EMG-contaminated, the gray bars represent the percentage of frontalis-contaminated trials correctly identified, and the light-gray bars represent the percentage of correctly identified fronto-tempo-contaminated trials.

from the 31 EMG-free trials. The goal was to select a decisive number that maximized the detection scheme's correct identification of EMG-contaminated trials (hits) and minimizes the incorrect identification of EMG-free trials as contaminated data (misses). We found that, independent of the decisive number used, 79% (15 of 19) of the frontalis-contaminated trials and 100% (12 of 12) of the fronto-tempo-contaminated trials were correctly identified. However, when the decisive number was 0, 1, 2, or 3, 16.1% (6 of 31) of the EMG-free trials were incorrectly identified as contaminated data. The number of misses decreased to 12.9% when the decisive number was set to 3, 4, or 5. Therefore, to minimize the number of misses, we selected 3 as the decisive number.

IV. Detection Accuracy

The proposed EMG detection scheme was designed using a subject's baseline, EMG-free data. However, in the case that such data is not available, we characterized the effect of EMG-contamination levels on the detection accuracy of our scheme. To do so, we computed the detection threshold using means and standard deviations from data that was 10, 20, 30, 40, and 50% contaminated by trials consisting of frontalis EMG and fronto-tempo EMG.

The detection threshold was computed 10 times from 30 EMG-free trials and a number of randomly selected contaminated trials. The number of contaminated trials was varied to achieve 10, 20, 30, 40, and 50% contamination levels. Then the mean of the 10 detection thresholds was used to classify all 62 trials (31 EMG-free, 19 frontalis-contaminated, and 12 fronto-tempo-contaminated). The results are shown in Fig. 4. At 10% contamination, 100% (12 of 12) detection of fronto-tempo contamination was observed, but frontalis-EMG detection was only 58% (11 of 19). For 20% or more EMG-contamination, the detection accuracy of frontalis-contaminated trials was between 25–35% and 35–50% for fronto-tempo-contaminated trials.

V. Discussion

Using the subject's baseline data, our detection scheme accurately identified 79% of frontalis-contaminated data, which was comparable to what was expected from the threshold we selected based on the histograms in Fig. 3. We expected to reject about 90% of fronto-tempo-contaminated trials, but instead exceeded expectations and rejected 100% of them. We also expected to incorrectly identify 20% of the EMG-free data as contaminated data. The improvements are due to the analysis of adjacent electrodes in addition to the primary ones, we falsely detected only 12% of the EMG-free trials.

In the case where the subject's baseline data was not available, our detection scheme did not mistake EMG-free data for contaminated data, but detection accuracy was fairly robust against 10% EMG contamination. At levels of 20% and higher, however, detection accuracy was approximately halved.

These results are not directly comparable with those reported in literature since these were preliminary results based on data from a single subject, but further work would allow for comparisons to be made.

It is worthwhile to note that our detection scheme is compatible with real-time EEG analysis applications, such as brain-computer interfaces (BCIs). The critical calculations in this scheme were computable by fast-fourier transform algorithms that can be performed in real time by current computer hardware. Also, the adjustable parameters for this method (the decisive number and the detection threshold) were determined based solely on baseline EEG data, which can be obtained an experiment and used during real-time analysis.

VI. Conclusion

The proposed EMG detection scheme used baseline EEG data to correctly identify 100% of fronto-tempo EMG-contaminated EEG trials, 79% of frontalis EMG-contaminated EEG trials, and falsely identified 12% of EMG-free trials as contaminated data. This performance exceeded the design expectations and was achieved without dedicated EMG recordings or prior knowledge of the frequency characteristics of the real-life EMG-contaminated data.

Future Work

Futher study on this topic would first entail an expansion of the detection performance of these methods to include more subjects and develop comparisons with results reported in the literature.

Also, tailoring this method and evaluating its performance during real-time EMG detection will be valuable toward real-time applications in EEG research such as BCIs and ictal detection.

Acknowledgment

The authors would like to thank the research staff and the physical therapists of the Cleveland FES Center at the Louis Stokes VAMC for their contributions to this study. This research was supported in part by the National Science Foundation under grants CISE IIS-0222743, EIA-0329811, and EIA-0423253, and US Dept. of Commerce under grant TOP-39-60-04003.

References

[1] T. Gasser, L. Stroka, and J. Mocks, "The transfer of EOG activity into the EEG for eyes open and closed." *Electroencephalography and Clinical Neurophysiology*, vol. 61, pp. 181–193, August 1985.

[2] C. Brunica, J. Moecks, and M. van den Berg-Lenssen, "Correcting ocular artifacts in the EEG: a comparison of several methods." *Journal of Psychophysiology*, vol. 73, pp. 72–83, July 1989.

[3] J. Barlow, "EMG artifact minimization during clinical EEG recordings by special analog filtering." *Electroencephalography and Clinical Neurophysiology.*, vol. 58, pp. 161–174, August 1984.

[4] T. Zikov, S. Bibian, G. A. Dumont, M. Huzmezan, and C. R. Ries, "A wavelet based de-noising technique for ocular artifact correction of the electroencephalogram." *Proceedings of the 24th Annual International Conference of the EMBS.*, vol. 1, pp. 98–105, October 2002.

[5] T. D. Lagerlund, F. W. Sharbrough, and N. E. Busacker, "Spatial filtering of multichannel electroencephalographic recordings through principal component analysis by singular value decomposition." *Brain Research: Cognitive Brain Research*, vol. 4, pp. 171–183, October 1997.

[6] T. Jung, S. Makeig, C. Humphries, T. Lee, M. J. McKeown, V. Iragui, and T. J. Sejnowski, "Removing electroencephalographic artifacts by blind source separation," *Psychophysiology*, vol. 37, pp. 163–178, March 2000.

[7] T. Gasser, J. Schuller, and U. Gasser, "Correction of muscle artefacts in the EEG power spectrum." *Clinical Neurophysiology*, vol. 116, pp. 2044–2050, June 2005.

[8] T. Platz, I. H. Kim, H. Pintschovius, T. Winter, A. Kieselbach, K. Villringer, K. R., and K. Mauritz, "Multimodal EEG analysis in man suggests impairment-specific changes in movement-related electric brain activity after stroke," *Brain*, vol. 123, pp. 2475–2490, December 2000.

[9] T. Platz, I. H. Kim, A. Engel, A. Kieselbach, and K. Mauritz, "Brain activation pattern as assessed with multi-modal EEG analysis predict motor recovery among stroke patients with mild arm paresis who receive the arm ability training." *Brain*, vol. 20, pp. 21–35, February 2002.

[10] J. J. Daly, Y. Fang, E. M. Perepezko, V. Siemionow, and G. Yue, "Prolonged cognitive planning time, elevated cognitive effort, and relationship to coordination and motor control following stroke," *IEEE Trans. Neural Syst. Rehab. Eng.*, June 2006, in press.

[11] P. Simon, May 2005, personal communication. Applications Engineer, Compumedics NeuroScan Ltd. (El Paso, TX).

[12] S.-L. Joutsiniemi, S. Kaski, and T. A. Larsen, "Self-organizing map in recognition of topographic patterns of EEG spectra," *IEEE Trans. Bio-Med. Eng.*, vol. 11, pp. 1062–8, November 1995.

[13] Brunner, "Muscle artifacts in the sleep EEG: automated detection and effect on all-night EEG power spectra." *Journal of Sleep Research*, vol. 5, pp. 155–164, September 1996.

[14] I. I. Goncharova, D. J. McFarland, T. M. Vaughan, and J. R. Wolpaw, "EMG contamination of EEG: spectral and topographical characteristics," *Clinical Neurophysiology*, vol. 114, pp. 1580–1593, March 2003.

[15] H. H. Jasper, "Report of the committee on methods of clinical examination in electroencephalography," *Electroencephalography and Clinical Neurophysiology.*, vol. 10, pp. 370–375, 1958.

[16] D. J. McFarland, L. M. McCane, S. V. David, and J. R. Wolpaw, "Spatial filter selection for EEG-based communication," *Electroencephalography and Clinical Neurophysiology.*, vol. 103, pp. 386–394, September 1997.

[17] J. Malmivuo and R. Plonsey, *Bioelectromagnetism*, 1st ed. New York, New York: Oxford University Press, 1995.